Microstructure and optical and electrical properties of TiO_2 nanotube thin films prepared by spin-coating method

Tana Bao[1,2] ✉, *Jun Ning*[1,2], *Altan Bolag*[1,2], *Narengerile Narengerile*[1,2]

[1]*College of Physics and Electronic Information, Inner Mongolia Normal University, Hohhot 010022, People's Republic of China*
[2]*Inner Mongolia Key Laboratory for Physics and Chemistry of Functional Materials, Inner Mongolia Normal University, Hohhot 010022, People's Republic of China*
✉ *E-mail: tanaph@imnu.edu.cn*

Published in Micro & Nano Letters; Received on 18th October 2018; Revised on 13th July 2019; Accepted on 30th July 2019

Titanium dioxide nanotubes prepared by hydrothermal method and the TiO_2 films and TiO_2 nanotube film were prepared by spin-coating method. The TiO_2 nanotube film and a part of TiO_2 film were annealed at 150°C for 1 h, while the another part of TiO_2 film was annealed at 500°C. The high-resolution transmission electron microscopy analysis indicated that the TiO_2 nanotubes prepared by hydrothermal method have been crystallised and the lattice plane indices corresponded to anatase {200}, and the TiO_2 nanotube grown along the ⟨100⟩ direction. The atomic force microscopy results show that the surface morphology of the TiO_2 film annealed at 150°C was smooth and uniform (0.62 nm in roughness) compared to the surface morphology of TiO_2 film annealed at 500°C (roughness is 2.41 nm). For the TiO_2 nanotube film, the nanotube fragments were uniformly dispersed in the base and the complete films have been prepared and the roughness was reached to 6.4 nm. The optical properties showed that the visible light transmittance of the TiO_2 nanotube film was larger (larger than 95%) than the TiO_2 film. The electrical properties showed that square resistance of TiO_2 nanotube film was smaller than that of TiO_2 film.

1. Introduction: In the face of the depletion of fossil energy and its pollution to the environment, new energy development for human civilization sustainable development provides important guarantees, of which solar photovoltaic is the most promising. Enhancing the photovoltaic conversion efficiency (PCE) of solar cells is the core research topic in the photovoltaic field.

The organic-inorganic hybrid halogen perovskite materials were first used in solar cells in 2009, when the photoelectric conversion efficiency was only 3.8% [1]. Within a few years development [2–6], the PCE of perovskite solar cells (PSCs) surpasses organic solar cells (14%) and dye-sensitised solar cells (13%) [7] and are expected to reach the efficiency of monocrystalline silicon solar cells (25.6%) [8]. With the renewal of efficiency records of PSCs, more and more attention has been paid to the stability, service life, replacement of heavy metal lead and fabrication of large-area flexible devices [9].

PSCs can be divided into meso-superstructured and planar heterojuction structures, each of which has a corresponding positive structure and inverted structure devices. Positive structure devices of PSCs are arranged as substrate/cathode/electron transport layer/perovskite absorption layer/hole transport layer/anode [10]. In order to improve the efficiency and life span of PSCs, various auxiliary layers are developed between perovskite absorption layer and electrodes. The electron transport layer is one of the most important auxiliary layer. An excellent electronic transmission material also has the function of enhancing electron injection and blocking hole transport. The most typical mesoscopic PSC is made of dense TiO_2 as electron transport material and mesoporous TiO_2 as the framework. After $CH_3NH_3PbX_3$ is grown on its surface, the p-type semiconducting material is deposited as the hole transport layer [11].

Titanium dioxide and its modification play an important role in solar cells and the generation of active free radicals under ultraviolet radiation [12]. In addition to the TiO_2 film [13–16], the TiO_2 nanotubes have large surface areas and higher photocatalytic degradation ability [17, 18]. In recent decades, one-dimensional (1D) highly ordered titanium dioxide nanotube arrays have been considered as one of the most promising photocatalytic materials [19, 20]. The important application of TiO_2nanotube arrays is solar cells. It is reported that Grimes and Mor [21] have fabricated dye-sensitised solar cells based on TiO_2 nanotube. The results show that if the length of TiO_2 nanotube arrays can reach several microns, the single-electron PCE of solar cells made of nanotubes can reach 31%. By measuring the voltage attenuation, it is found that nanotubes are more conducive to the internal transmission of electrons than nanocrystals [22]. The preparation methods of TiO_2 nanotubes include template method [23], hydrothermal method [24] and anodic oxidation method [25]. Template method and anodic oxidation method can prepare ordered titanium dioxide nanotubes, but the process is complex, the productivity is low and the cost is high. The TiO_2 nanotubes prepared by hydrothermal method have low order but low cost. Many previous studies have been based on ordered titanium dioxide nanotubes.

However, little research has been done on disordered titanium dioxide nanotubes, especially in PSC. In this Letter, in order to develop more stable and electronic transmission efficient PSCs, we use TiO_2 nanotube film as electron transport layer instead of TiO_2 film and try to obtain high transmittance and low resistivity by studying its microstructure, morphology, optical and electrical properties.

2. Experiment

2.1. Preparation of samples: First, the TiO_2 nanopowder was prepared by sol–gel method. The analytical reagents (AR) tetrabutyl titanate (Beijing Chemical Reagent Co. LTD), AR grade absolute alcohol (Sinopharm Group) and 36 vol% acetic acid (Tianjin Fengchuan Chemical Reagent Technology Co. LTD) were used as starting materials to prepare titania powder and then the dried gel was annealed for 2 h at 600°C.

Second, the TiO_2 nanotubes were prepared by hydrothermal reaction. The NaOH 12.5 g of 96 mol% (Tianjin Fengchuan Chemical Reagent Technology Co. LTD) was added to the deionised water of 30 ml to produce strong alkali solution. Then 0.3 g TiO_2 nanopowder was mixed with strong alkali. The mixed

doi: 10.1049/mnl.2018.5642

liquid was stirred for 30 min in a constant temperature magnetic stirrer. After mixing, the mixture was put into the reactor and kept in the drier at 140°C for 16 h. After cooling to room temperature, the reactant was poured into a centrifuge tube. Centrifugation was performed to separate the lye from the solid material. After separation, the nanotubes were extracted and put into a beaker, washed with deionised water to neutral, then washed with hydrochloric acid to form flocculent, then washed with deionised water until neutral, and then dried in a drier for 24 h.

The TiO_2 nanotube films were prepared by high-speed spin-coating method (speed 1500 rpm, time 30 s). 0.3 ml of 98 mol% titanium diisopropoxide bis (acetylacetonate) (Adamas-beta) solution and 3.5 ml ethanol were mixed in small bottles and stirred for 30 min at room temperature to get the titanate solution (TAA). 1.2 mg TiO_2 nanotubes were added into 1.2 ml ethanol and stirred for 30 min at room temperature to get the TiO_2 nanotube solution. The TiO_2 nanotubes solution need to be further diluted to 1/10, i.e. 20 µl TiO_2 nanotubes solution was dripped with 180 µl TAA sols, and then dispersed in an ultrasonic instrument for 10 min. Three dried sodium calcium slides were labelled with 1, 2 and 3. Slides 1 and 2 were added with TAA sol and slide 3 was added with TiO_2 nanotube sol to prepare thin films. The samples of labelling 1 and 2 were annealed at 150 and 500°C for 1 h, respectively, and the sample of labelling 3 was annealed at 150°C for 1 h.

2.2. Measurement: The phase composition of TiO_2 film and nanopowders were analysed by an X-ray diffraction (XRD, PW1830) using copper Ka radiation and the scanning angles ranged from 2θ of 20° to 80° at steps of 0.02°.

The morphology, interplanar spacing and orientation of the TiO_2 nanotube were characterised using high-resolution transmission electron microscopy (HRTEM, JEM-2100F, JEOL) with a point resolution of 0.19 nm, lattice resolution of 0.14 nm and an operating voltage of 200 kV. The TiO_2 nanotube was diluted by absolute alcohol and dropped on a carbon film supported by a copper grid.

The surface morphology of the TiO_2 film was analysed by atomic force microscopy (AFM, S-3400N, HITACHI), the optical properties were measured by ultraviolet-visible spectrophotometer (722, Shanghai Yoke Instrument Co., LTD) and the electrical property was measured by four-probe resistivity tester (ST2253, Suzhou Lattice Electronics Co. LTD).

3. Results and discussion

3.1. XRD measurements: Fig. 1 illustrates the XRD patterns of the TiO_2 films and powders. It can be seen from Fig. 1*a* that there are no obvious crystal peaks in the three groups of samples; they are amorphous diffuse peaks. Fig. 1*b* illustrates the XRD patterns of the TiO_2 nanopowders annealed at 600°C. This indicates that anatase has been crystallised, and a very small amount of rutile exists in it. Compared with the XRD pattern of the nanopowder in Fig. 1***b***, the nano-tube film has been amorphous, indicating that the anatase in the nanopowder becomes amorphous when annealed at 150°C.

For the TAA films, no crystallisation was found after annealing at 150 and 500°C. It shows that TAA thin films cannot crystallise even at 500°C annealing.

3.2. Transmission electron microscopy (TEM)/HRTEM measurements: The TiO_2 nanopowders were prepared by sol–gel method and the morphology of the TiO_2 nanopowders was studied with TEM. It can be seen from Fig. 2*a* that the TiO_2 has been crystallised and the diameter is only about 15–30 nm.

Fig. 2*b* shows the typical crystallisation images of TiO_2 nanopowders, the d-spacing of the most of the grain is measured to 3.5 and 2.3 Å, the lattice plane indices corresponded to anatase {101} and {004}, the crystal zone axis is [010].

The TiO_2 nanotubes were prepared by hydrothermal method with self-made titanium dioxide nanoparticles and the microstructure and morphology of the TiO_2 nanotube was studied by TEM. It can be seen from Fig. 3*a* that the TiO_2 nanotubes with hollow have been formed. The diameter of nanotube was only 8–15 nm and the length was about 70–240 nm.

HRTEM analysis shows the microsturcture of TiO_2 nanotubes wall in Fig. 3*b*. The d-spacing of the nanotube wall measured to 1.98 Å and the lattice plane indices corresponded to anatase {200}. In embedded graph in the lower right corner of Fig. 3*b*, four pairs of electron diffraction spots were observed and the d-spacing of each pair of spots were measured clockwise to 1.98, 1.40, 1.97 and 1.41 Å. The angle between the first and third electron diffraction spots was ~90° and, the angle between the first and second electron diffraction spots was ~45°, the angle between the third and fourth electron diffraction spots was ~45°. As TiO_2 belongs to the tetragonal system, those four lattice plane indices corresponded to anatase (020), (220), (200), (2$\bar{2}$0), respectively, and the crystal zone axis is [001], which were consistent with the values reported for JCPDS Card No. 89-4921. Therefore, we cannot see the {101} characteristic lattice planes which often appear in TiO_2 nanopowders.

We deduced that the growth direction of TiO_2 nanotube is ⟨100⟩ direction. It may be because the (100)/(010) surface of the anatase reveals a more relaxed atomic arrangement and the surface formation energy was 0.53 J/m^2, which was lower than the surface formation energy of (001) face (0.9 J/m^2) [26]. So, the anatase nanotube was grown along the [100]/[010] axis. Another hand, we can see the d-spacing of {200} and {220} were 1.98 and 1.40 Å, respectively, which is larger than that of the standard values 1.89 and 1.34 Å (JCPDS Card No. 89-4921). It may be because the lattice was extended along the ⟨100⟩ direction when the nanotube was growing quickly.

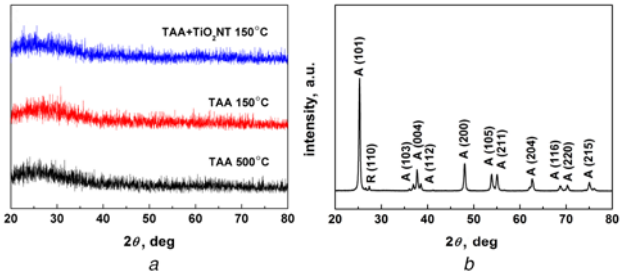

Fig. 1 *XRD pattern of*
a TAA and TAA + TiO_2 nanotube films annealed at 150°C
b TiO_2 nanopowder annealed at 600°C

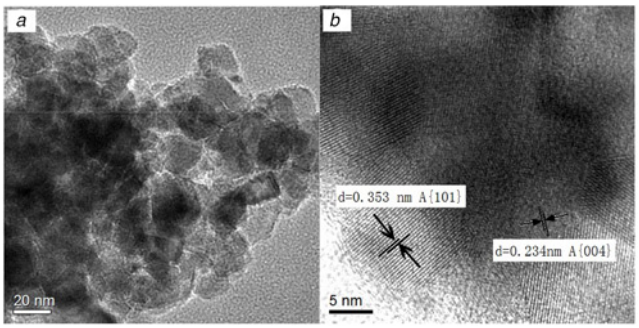

Fig. 2 *TEM image of TiO_2 nanopowders prepared by*
a Sol–gel method
b HRTEM image

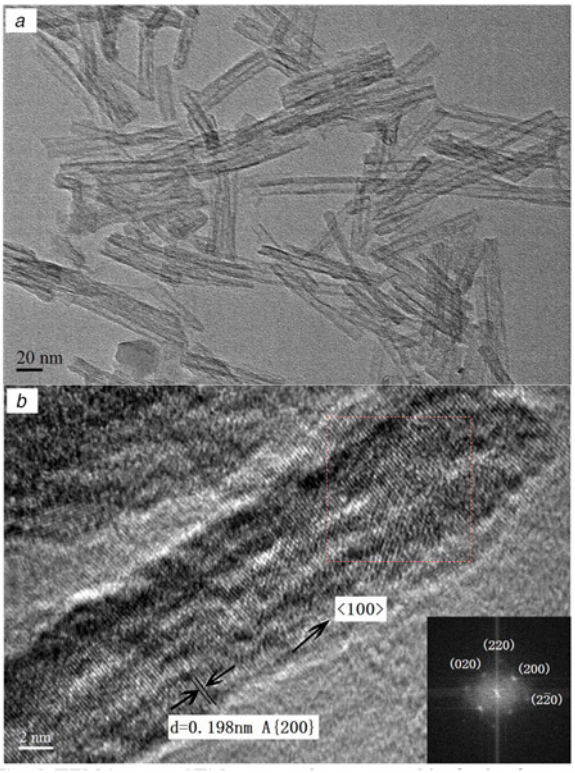

Fig. 3 *TEM image of TiO_2 nanotube prepared by*
a Hydrothermal reaction
b HRTEM image

First, the hydrothermal synthesis of titanium dioxide nanotubes has low cost and high efficiency. However, although the titanium dioxide prepared by hydrothermal method is disordered, its structure is controllable because of its preferred growth direction, which is conducive to electron transport.

3.3. AFM measurements: In order to study the surface morphology and roughness of TiO_2 nanofilms, the AFM was used to analyse the surface morphology and roughness of three groups of samples. Fig. 4 characterises the surface morphology and the 3D profile of the sample.

The surface roughnesses of the sample were shown in Table 1.

It can be seen from Figs. 4*a* and *b*, the surface of the TAA film annealed at 500°C is not smooth as the distribution of the film is inhomogeneous and not compact, and even appeared holes on the surface. Another way, the roughness of it was larger compared with the samples annealed at 150°C (Table 1). However, the surface morphology of TAA film annealed at 150°C (Figs. 4*c* and *d*) is smooth, uniform and compact, and the surface roughness is only 0.62 nm (Table 1). The TAA + TiO_2 nanotube films (Figs. 4*e* and *f*) annealed at 150°C have uniform substrate, but the average roughness is about 6.4 nm (Table 1) due to the addition of TiO_2 nanotubes. There are distinct fragments on the surface. In Fig. 4*e*, the small black spots in the centre of each fragment correspond to the hollow of nanotubes. Although there are nanotube fragments on the surface, the film surface still has good continuity, and there are no holes and other defects.

The results of AFM show that the electronic transport layer of TAA film and TAA + TiO_2 film prepared by spin-coating method has better morphology and coverage even after low-temperature annealing, which is very effective for reducing cost.

3.4. Optical and electrical measurement: The light absorption/transmission data of the sample were shown in Table 2. It can be seen from the table that the ultraviolet light absorption is lower and the light transmission is higher for the TAA film annealed at 150°C compared to the TAA film annealed at 500°C. In addition, the TAA + TiO_2 nanotube film (150°C) has the lowest UV absorption than other samples. It shows that the properties of the TiO_2 sol film treated at low temperature are better than that which are treated at high temperature when used as electron transport layer material of the PSCs. Compared with the three samples, the TiO_2 nanotube film demonstrated good optical quality as it displays highest average transmittance (91.31–97.60%) in the visible region.

In Table 3, one can see that the ultraviolet absorption peak of TiO_2 nanotubes is slightly red-shifted compared with that of TiO_2

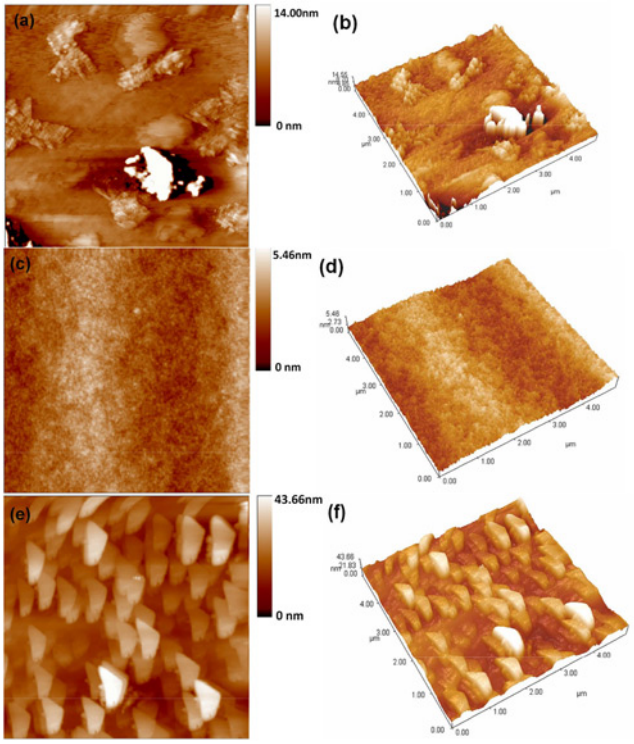

Fig. 4 *AFM surface morphology and the 3D profile of TAA films*
a, b TAA films, 500°C
c, d TAA films, 150°C
e, f TAA + TiO_2 nanotube films

Table 1 Surface roughness of the TiO_2 thin films

	TAA films, 500°C	TAA films, 150°C	TiO_2 NT films, 150°C
roughness sq., nm	2.41	0.62	6.40

Table 2 Light absorption/transmission data of TiO_2 nanofilms

		400 nm	500 nm	600 nm	700 nm	800 nm
A	TAA, 500°C	0.072	0.040	0.026	0.019	0.015
	TAA, 150°C	0.056	0.037	0.028	0.021	0.016
	TiO_2 NT, 150°C	0.039	0.022	0.016	0.013	0.010
T, %	TAA, 500°C	84.69	91.14	94.05	95.71	96.65
	TAA, 150°C	87.78	91.76	93.86	95.33	96.34
	TiO_2 NT, 150°C	91.31	95.16	96.39	97.10	97.60

doi: 10.1049/mnl.2018.5642

Table 3 Light absorption peak of TiO_2 nanofilms

Sample	Absorption peak, nm	bandgap, eV
TAA, 500°C	383.2	3.24
TAA, 150°C	383.2	3.24
TiO_2 NT, 150°C	384.9	3.22

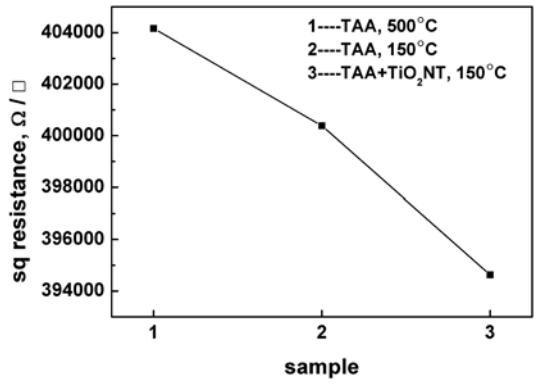

Fig. 5 *Square resistance of TiO_2 nanofilms*

thin films (TAA 383.2 nm to TiO_2 NT 384.9 nm). The bandgap decreases from $E_g = 3.24$ eV in thin films to $E_g = 3.22$ eV in nanotubes. The TiO_2 nanotube can bring out its absorption edge red-shift slightly, broaden light response range to visible light region, which result in the enhancement in visible light photoactivity.

Due to its unique tubular structure and good light scattering effect, titanium dioxide nanotubes exhibit extremely high photon capture efficiency, and tubular structure provides the transmission of photogenerated electrons. However, the red shift is not obvious because the nanotubes are not arranged in an orderly manner, and their lengths are uneven. Some nanotubes are only 70–80 nm long (Fig. 3).

In order to study the electrical properties of TiO_2 thin films, the square resistance of the films was measured by a digital four-probe tester. The results are shown in Fig. 5. The resistivity of the three samples is higher than that of the materials needed for the electron transport layer of the solar cell. This may be due to the fact that the thin films are prepared on non-conductive ordinary slide, and there is obviously room for improvement in technology. However, we can still see the variation of the square resistance of different films. The resistance of the TiO_2 sol film annealed at 500°C is the largest, as of another TiO_2 sol film annealed at 150°C is second. Among the three, the square resistance of the TAA + TiO_2 nanotube film is the smallest. It is clear that the electrical property of the thin films with the addition of TiO_2 nanotubes is improved to a certain extent.

The reason may be that for semiconductor materials, the high carrier concentration of materials with narrow bandgap necessarily leads to the conductivity of nanotubes being better than that of nanofilms (Table 3). Semiconductor resistivity is proportional to carrier mobility and bandgap [27].

The above results show that even annealed at low temperature, the transmission and conductivity of TAA thin films and TAA + TiO_2 nanotube thin films are better, and the performance of nano-titanium dioxide thin films is the best. Therefore, the TiO_2 nanotubes film is more suitable to be used as the electron transport layer of PSCs compared to the TAA films.

4. Conclusions: In this Letter, the TiO_2 nanotubes were prepared by low-cost hydrothermal method, and TiO_2 nanofilms were prepared by spin-coating method.

The nano-TiO_2 thin films show amorphous diffuse scattering peaks after annealed at 150 and 500°C; the TiO_2 nanotube film becomes amorphous after annealed at 150°C.

The crystal zone axis of TiO_2 nanoparticles was [010], while the crystal zone axis of TiO_2 nanotubes was [001]. The TiO_2 nanotube is grown along the ⟨100⟩ direction as the surface formation energy of the anatase (100)/(010) face was lower than the surface formation energy of (001) face. The lattice was extend along the ⟨100⟩ direction when the nanotube was growing. So, its structure is controllable because of its preferred growth direction, which is conducive to electron transport.

The AFM morphology of TAA films annealed at 150°C is more compact and homogeneous than that of TAA annealed at 500°C and the surface roughness is 0.62 nm. The TiO_2 film has better morphology and coverage even after low-temperature annealing and the TAA + TiO_2 nanotube films have good continuity although it is composed of the disordered nanotube which is prepared by hydrothermal method.

The light transmittance of the films added with TiO_2 nanotubes is the best (larger than 95%). The ultraviolet absorption peak of titanium dioxide nanotubes is slightly red-shifted compared with that of titanium dioxide thin films. The bandgap of anatase decreases from $E_g = 3.24$ eV in thin films to $E_g = 3.22$ eV in nanotubes. The device can be guaranteed to be more stable under ultraviolet radiation and have better optical performance.

The square resistance of films added with TiO_2 nanotubes was minimal and the electron transport efficiency is higher. Samples added with TiO_2 nanotubes have been improved significantly in the photo and electric properties compared to the TAA films. The transmission and conductivity of TiO_2 thin films annealed at low temperature (150°C) are better than annealed at high temperature (500°C). It is very effective for reducing cost.

5. Acknowledgments: This work was supported by the Natural Science Foundation of Inner Mongolia (grant nos. 2015BS0515 and 2018MS02011); National Nature Science Fund Project (grant no. 21762033 and grant no. 21663018).

6 References

[1] Kojima A., Teshima K., Shirai Y., *ET AL.*: 'Optical analysis in $CH_3NH_3PbI_3$ and $CH_3NH_3PbI_2Cl$ based thin-film perovskite solar cell', *J. Am. Chem. Soc.*, 2009, **131**, pp. 6050–6051

[2] Im J.H., Lee C.R., Lee J.W., *ET AL.*: 'Efficient perovskite quantum-dot-sensitized solar cell', *Nanoscale*, 2011, **3**, pp. 4088–4093

[3] Kim H.S., Lee C.R., Im J.H., *ET AL.*: 'Lead iodide perovskite sensitized all-aolid-statesubmicron thin film mesoscopic solar cell with efficiency exceeding 9%', *Sci. Rep.*, 2012, **2**, p. 591

[4] Burschka J., Pellet N., Moon S.J., *ET AL.*: 'Sequential deposition as a route to high-performance perovskite-sensitized solar cells', *Nature*, 2013, **499**, pp. 316–319

[5] Liu M.Z., Johnston M.B., Snaith H.J.: 'Efficient planar heterojunction perovskite solar cells by vapour deposition', *Nature*, 2013, **501**, pp. 395–398

[6] Zhou H.P., Chen Q., Li G., *ET AL.*: 'Interface engineering of highly efficient perovskite solar cells', *Science*, 2014, **345**, p. 542

[7] Ting H.K., Ni L., Ma S.B., *ET AL.*: 'Progress in electron-transport materials in application of perovskite solar cells', *Acta Phys. Sin*, 2015, **64**, pp. 038802-1–038802-11

[8] Service R.F.: 'Perovskite solar cells keep on surging', *Science*, 2014, **344**, p. 458

[9] Meroni S.M.P., Mouhamad Y., De Rossi F., *ET AL.*: 'Homogeneous and highly controlled deposition of low viscosity inks and application on fully printable perovskite solar cells', *Sci. Technol. Adv. Mater.*, 2018, **19**, pp. 1–9

[10] Cui J., Yuan H.L., Li J.P., *ET AL.*: 'Recent progress in efficient hybrid lead halide perovskite solar cells', *Sci. Technol. Adv. Mater.*, 2015, **16**, pp. 036004-1–036004-14

[11] Loi M.A., Hummelen J.C.: 'Hybrid solar cells: perovskites under the sun', *Nat. Mater.*, 2013, **12**, pp. 1087–1089

[12] Thompson T.L., Yats J.T.: 'Surface science studies of photoactivation of TiO_2 new photochemical process', *Chem. Rev.*, 2006, **106**, pp. 4428–4453

[13] Evtushenko Yu.M.: 'Optical properties of TiO_2 thin films', *Phys. Proc.*, 2015, **73**, pp. 100–107
[14] Chen H., Liu G., Wang L.: 'Switched photocurrent direction in Au/TiO_2 bilayer thin films', *Sci. Rep.*, 2015, **5**, pp. 10852-1–10852-9
[15] Xing J., Wei H., Guo E.J., *ET AL.*: 'Highly sensitive fast-response UV photodetectors based on epitaxial tiO_2 films', *J. Phys. D, Appl. Phys.*, 2011, **44**, pp. 375104–375109
[16] Bogle K.A., More K.D., Dadge J.W., *ET AL.*: 'Nano-crystalline TiO_2 thin film: synthesis and investigation of its optical switching characteristics', *Thin Solid Films*, 2018, **653**, pp. 62–66
[17] Chien C.T., Hsisheng T.: 'Structural features of nanotubes synthesized from NaOH treatment on TiO_2 with different post-treatments', *Chem. Mater.*, 2006, **18**, pp. 367–373
[18] Cheng K.Y., Cai Z.Q., Fu J., *ET AL.*: 'Synergistic adsorption of Cu(II) and photocatalytic degradation of phenanthrene by a jaboticaba-like TiO_2/titanate nanotube composite: an experimental and theoretical study', *Chem. Eng. J.*, 2019, **358**, pp. 1155–1165
[19] Xu Z., Liu Y., Ren F., *ET AL.*: 'Development of functional nanostructures and their applications in catalysis and solar cells', *Coordin. Chem. Rev.*, 2016, **320-321**, pp. 153–180
[20] Wang G., Zhang Q.Z., Chen Q.H.: 'Photocatalytic degradation performance and mechanism of dibutyl phthalate by graphene/TiO_2 nanotube array photoelectrodes', *Chem. Eng. J.*, 2019, **358**, pp. 1083–1090
[21] Grimes C.A., Mor G.K.: 'Use of highly-ordered TiO_2 nanotube arrays in dye-sensitized solar cells', *Nano Lett.*, 2006, **6**, pp. 215–218
[22] Mor G.K., Karthik S., Paulose M., *ET AL.*: 'Use of highly-ordered TiO_2 nanotube arrays in dye-sensitized solar cells. *Nano Lett.*, 2006, **6**, (2), pp. 215–218
[23] Liu F.F., Li X.Y., Zhao Q.D., *ET AL.*: 'Structural and photovoltaic properties of highly ordered $ZnFe_2O_4$ nanotube arrays fabricated by a facile sol-gel template method. *Acta Mater.*, 2009, **57**, (9), pp. 2684–2690
[24] Sreekantan S., Wei L.C.: 'Study on the formation and photocatalytic activity of titanate nanotubes synthesized via hydrothermal method. *J. Alloys Compounds*, 2010, **490**, (1), pp. 436–442
[25] Valota A., LeClere D.J., Skeldon P., *ET AL.*: 'Influence of water content on nanotubular anodic titania formed in fluoride /glycerol electrolytes', *Electrochim. Acta*, 2009, **54**, (18), pp. 4321–4327
[26] Diebold U.: 'The surface science of titanium dioxide', *Surf. Sci. Rep.*, 2003, **48**, pp. 53–229
[27] Yang B.C.: 'Thin film physics and technology' (Chengdu University of Electronic Science and Technology Press, People's Republic of China, 1994)

doi: 10.1049/mnl.2018.5642